Taylor & Francis
Taylor & Francis Group

Amyotrophic Lateral Sclerosis and Frontotemporal Degeneration

ISSN: 2167-8421 (Print) 2167-9223 (Online) Journal homepage: http://www.tandfonline.com/loi/iafd20

Proteomic profiling of the spinal cord in ALS: decreased ATP5D levels suggest synaptic dysfunction in ALS pathogenesis

Jooyeon Engelen-Lee, Anna M. Blokhuis, Wim G. M. Spliet, R. Jeroen Pasterkamp, Eleonora Aronica, Jeroen A. A. Demmers, Roel Broekhuizen, Giovanni Nardo, Niels Bovenschen & Leonard H. Van Den Berg

To cite this article: Jooyeon Engelen-Lee, Anna M. Blokhuis, Wim G. M. Spliet, R. Jeroen Pasterkamp, Eleonora Aronica, Jeroen A. A. Demmers, Roel Broekhuizen, Giovanni Nardo, Niels Bovenschen & Leonard H. Van Den Berg (2017) Proteomic profiling of the spinal cord in ALS: decreased ATP5D levels suggest synaptic dysfunction in ALS pathogenesis, Amyotrophic Lateral Sclerosis and Frontotemporal Degeneration, 18:3-4, 210-220, DOI: 10.1080/21678421.2016.1245757

To link to this article: http://dx.doi.org/10.1080/21678421.2016.1245757

Published online: 29 Nov 2016.

Amyotrophic Lateral Sclerosis and Frontotemporal Degeneration, 2017; 18: 210–220

Taylor & Francis
Taylor & Francis Group

RESEARCH ARTICLE

Proteomic profiling of the spinal cord in ALS: decreased ATP5D levels suggest synaptic dysfunction in ALS pathogenesis

JOOYEON ENGELEN-LEE[1]*, ANNA M. BLOKHUIS[2]*, WIM G. M. SPLIET[3], R. JEROEN PASTERKAMP[2], ELEONORA ARONICA[4], JEROEN A. A. DEMMERS[5], ROEL BROEKHUIZEN[3], GIOVANNI NARDO[6], NIELS BOVENSCHEN[3,7]† & LEONARD H. VAN DEN BERG[8]†

[1]Department of Neurology, Academic Medical Centre, Amsterdam, The Netherlands, [2]Department of Translational Neuroscience, Brain Centre Rudolf Magnus, University Medical Centre Utrecht, Utrecht, The Netherlands, [3]Department of Pathology, University Medical Centre Utrecht, Utrecht, The Netherlands, [4]Department of (Neuro)Pathology, Academic Medical Centre, Amsterdam, The Netherlands, [5]Proteomics Centre, Erasmus University Medical Centre, Rotterdam, The Netherlands, [6]Department of Molecular Biochemistry and Pharmacology, Mario Negri Institute for Pharmacological Research, Milano, Italy, [7]Laboratory of Translational Immunology, University Medical Centre Utrecht, Utrecht, The Netherlands, and [8]Department of Neurology and Neurosurgery, Brain Centre Rudolf Magnus, University Medical Centre Utrecht, Utrecht, The Netherlands

Abstract

Background: We aimed to gain new insights into the pathogenesis of sporadic ALS (sALS) through a comprehensive proteomic analysis. *Methods*: Protein profiles of the anterior and posterior horn in post-mortem spinal cord samples of 10 ALS patients and 10 controls were analysed using 2D-differential gel electrophoresis. The identified protein spots with statistically significant level changes and a spot ratio >2.0 were analysed by LC-MS/MS. *Results*: In the posterior horn only 3 proteins were differentially expressed. In the anterior horn, 16 proteins with increased levels and 2 proteins with decreased levels were identified in ALS compared to controls. The identified proteins were involved in mitochondrial metabolism, calcium homeostasis, protein metabolism, glutathione homeostasis, protein transport and snRNP assembly. The two proteins with decreased levels, ATP5D and calmodulin, were validated by Western blot and immunostaining. Immunohistochemical and immunofluorescent double staining of ATP5D and synaptophysin showed that the reduction of ATP5D was most pronounced at synapses. *Conclusions*: We speculate that mitochondrial dysfunction in synaptic clefts could play an important role in sALS pathogenesis. A similar approach revealed decreased calmodulin expression mainly in the neuronal body and dendrites of ALS patients. These findings contribute to a deeper understanding of the disease process underlying ALS.

Key words: *Amyotrophic lateral sclerosis*, *Two-Dimensional Differential Gel Electrophoresis (2D-DIGE)*, *spinal cord*, *proteomics*, *ATP5D*, *synaptic mitochondrial defect*

Introduction

With an average incidence of 3/100,000 per year, amyotrophic lateral sclerosis (ALS) is the most common motor neuron disease. ALS is characterised by selective degeneration of motor neurons in the primary motor cortex, brain stem and anterior horn of the spinal cord. Patients suffer from progressive muscle weakness, eventually leading to respiratory failure and death, on average within three to five years. The majority of cases have no family history of the disease and are said to be sporadic (sALS).

The cause of ALS remains to be identified, although many pathogenic mechanisms have been suggested and investigated, including oxidative

*These authors contributed equally (shared first authors).
†These authors contributed equally (shared last authors).
Correspondence: L. H. ven den Berg, Department of Neurology and Neurosurgery, Brain Centre Rudolf Magnus, University Medical Centre Utrecht, Utrecht, The Netherlands Tel: +31 88 755 7939. E-mail: L.H.vandenBerg@umcutrecht.nl

(Received 21 May 2016; revised 22 September 2016; accepted 25 September 2016)

ISSN 2167-8421 print/ISSN 2167-9223 online
DOI: 10.1080/21678421.2016.1245757

stress, glutamate excitotoxicity and protein aggregation (1). However, the cause of the motor neuron-specific degeneration observed in ALS is far from being unravelled. Several genes in familial ALS (fALS) and many susceptibility genes in sALS have been implicated in the disease (2). Many of the proteins encoded by these genes are found in protein aggregates in ALS-degenerated motor neurons, a pathological hallmark of the disease (3). Cellular processes regulated by ALS-associated gene alterations point to mitochondrial function (SOD1), RNA processing (FUS, TARDBP, ATXN2, C9orf72), protein turnover (UBQLN2, OPTN) and cellular transport (PFN1, TUBA2) (4). As yet, there is no coherent model of pathogenesis. Although many attempts have been undertaken to identify genetic alterations associated with ALS, studies investigating proteomic alterations are relatively rare. However, examining protein profiles in human tissue using mass spectrometry has the potential to identify new proteins involved in disease pathogenesis.

In the present study, we investigated the proteome of the anterior and posterior horn of spinal cord tissue from 10 human sALS cases and 10 controls using 2D-DIGE to discover cellular pathways that are disrupted in the disease.

Materials and methods

Sample preparation

The study included 10 patients with ALS and 10 control subjects. The characteristics of patients and controls are listed in Table 1. None of the patients had a family history of ALS or FTD, and known disease-causing mutations in *SOD1*, *TARDBP*, *FUS*, *VCP*, *OPTN*, *UBQLN2* or *C9ORF72* were excluded. Cervical, thoracic (high and low) and lumbar levels of post-mortem spinal cords were collected in liquid nitrogen and stored at -80 °C. In parallel, spinal cords were processed to obtain formalin-fixed, paraffin-embedded (FFPE) tissue for histological, immunohistochemical and immunofluorescent examination. The ALS spinal cords showed typical characteristics of ALS: decrease of motor neurons (25% decrease), Bunina bodies, ubiquitin-positive inclusions, bleaching of pyramidal tract and an increase of microglia (see Figure 1). About 0.015-0.065 gram of anterior horn and posterior horn tissue was isolated using a 2 or 3 mm skin biopsy punch (Figure 1) from 3-5 mm thick slices of lumbosacral spinal cord segments (except for one ALS case in which the material was obtained from a cervical segment because other levels of spinal cord were not available).

Fluorescent 2-dimensional difference gel electrophoresis

From the anterior horns, protein was extracted with a mean protein extraction efficiency of 4.63 μg/mg in the ALS group and 4.85 μg/mg in the control group. From the posterior horn of ALS patients and controls, protein was extracted with mean protein extraction efficiencies of 5.38 μg/mg and 5.31 μg/mg, respectively. The tissue samples were cut into small pieces and suspended in lysis buffer (400 μL/0.05 gram) composed of 150 mM NaCl, 1% NP-40 and 50 mM Tris pH 7.4. After 5 hours of incubation at 4 °C, 100 μg of protein was precipitated using the 2D-CleanUp kit (GE Healthcare) according to the manufacturer's instructions. The samples from the ALS and control group were labelled with 400 pmol of Cy3 or Cy5, and a pooled sample of equal amounts of protein from each experimental sample was labelled with Cy2, as described previously (5). Randomly paired samples (100 μg per sample) were combined and, together with the Cy2 labelled

Table 1. Summary of characteristics of ALS cases and controls used in the study.

	ALS	Controls
Number	10	10
% Female	40%	50%
Mean age at death (SD)	62.6 (10.6)	67.0 (14.2)
Age at onset	57.6 (10.9)	
Site of onset		
Bulbar	5	
Cervical	4	
Thoracical	0	
Lumbosacral	1	
El-Escorial criteria		
Definite	1	
Probable	5	
Probable LS	0	
Possible	4	
ALS-plus (Extrapyramidal signs/FTD)	0	
Cause of death	Respiratory failure	Sepsis, chronic lymphatic leukaemia, cardiac tamponade, subarachnoid bleeding, carcinoma (prostate, colorectal, oesophagus, bladder), pancreatitis, aorta dissection

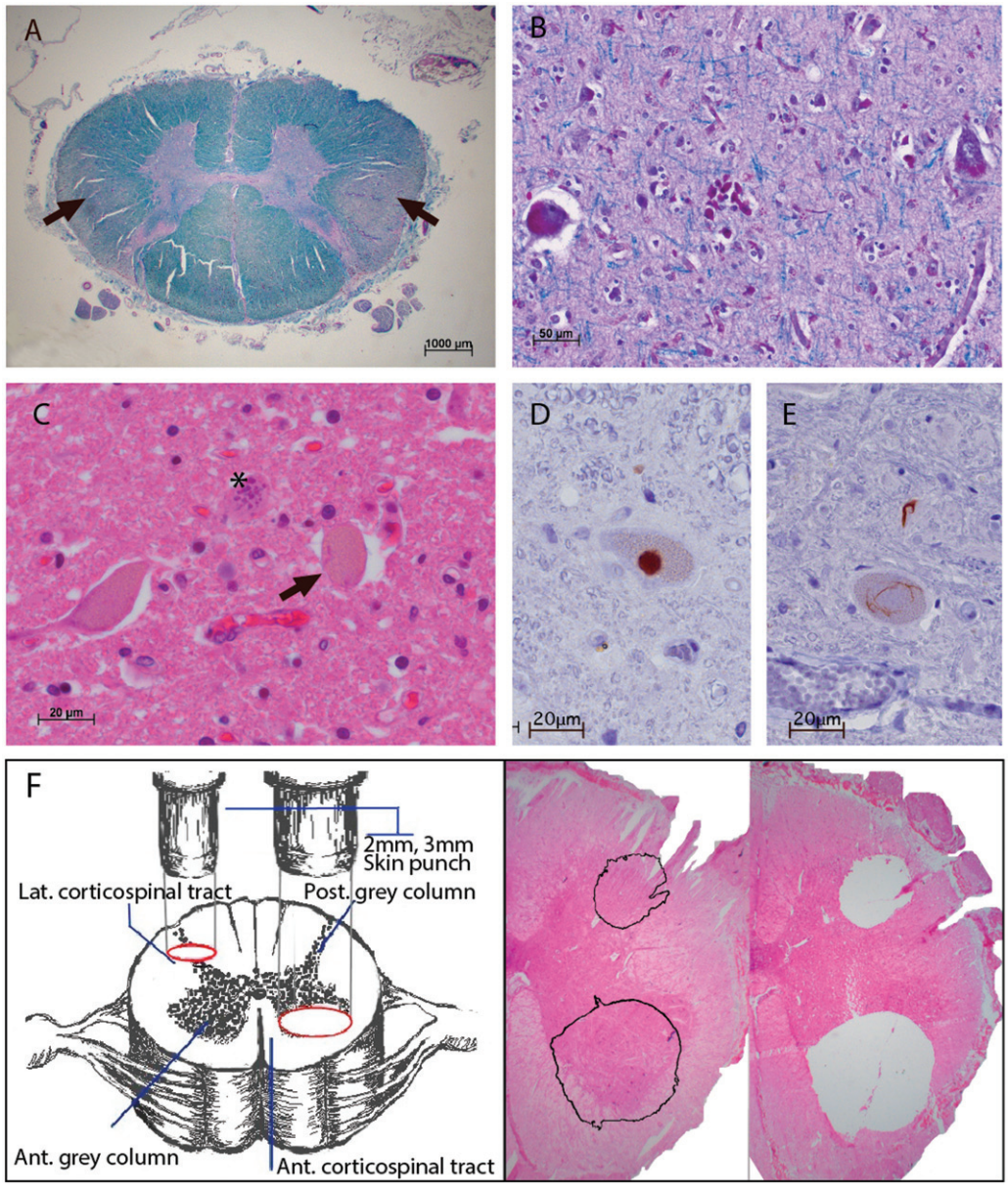

Figure 1. (A) L-PAS staining of thoracic ALS spinal cord showing demyelinisation of the lateral corticospinal tract. (B) L-PAS staining of ALS motor cortex. A degenerated neuron is cleared by a group of microglia. (C) hematoxyline-eosine (HE) staining of the spinal cord anterior horn showing a degenerated motor neuron (arrow) and the presence of Bunina bodies (asterix). (D) p-62 staining of a round inclusions and (E) ubiquitin-staining of a skein-like inclusion. (F) Isolation of the anterior and posterior horn of the spinal cord using a skin biopsy punch. Right panel shows HE-stained spinal cord of an ALS patients before and after skin biopsy punch.

internal standard, separated by 2D gel electrophoresis (5). Dye swaps were included to exclude preferentially labelled proteins from the analysis: in 6 out of 10 runs, ALS samples were labelled with Cy3 and control samples with Cy5, and in 4 out of 6 runs, ALS samples were labelled with Cy5 and control samples with Cy3 (see Supplementary Table 1 for an overview of sample combinations and Cy-labels). Relative quantification of matched gel features was performed by using Decyder DIA and BVA software (GE Healthcare, Waukesha, WI). For inter-gel analyses, the internal standard method was used. By using an internal standard, abundance of each protein spot can be measured relative to the corresponding spot in the internal standard, allowing for accurate quantitation and statistical comparison between gels (6). Statistical analysis of gel spot volume quantification was performed using the Student's *t*-test. Proteins were regarded as significantly different if (1) they differed at least 2.0-fold in fluorescence volume intensity, (2) the difference was statistically significant ($p < 0.05$), and (3) they could be detected in at least 3 patients.

Mass spectrometry

Differential protein spots were picked from a separate 'pick' gel, loaded with a pooled sample of equal amounts of protein from each experimental sample (Supplementary Table 2). 2D SDS-PAGE gel spots were subjected to in-gel reduction with dithiothreitol, alkylation with iodoacetamide and digestion

Table 2. Overview of proteins with significant level changes in the anterior horn of ALS; upregulated proteins have a positive, and downregulated negative log2 fold change values, respectively.

Biological process	Spot no.	Mascot score	Number of unique peptides/total peptides	Log2 fold change (ALS/control)	T-test p-value	Gene symbol	Protein name	Chromosome locus	pI	Mw
Calcium homeostasis	700	121	2/2	2.00	0.028	RCN1	Reticulocalbin 1	11p13	4.68	35845
	1392	338	7/9	2.04	0.0042	CHP1	Calcineurin B homologous protein 1	15q13.3	4.98	22311
	1550/1588	110/323	2/3 5/11	−2.59/ −2.12	0.00082/ 0.00048	CALM1	Calmodulin	14q24-q31	4.09	16695
Protein metabolism	171	1641	25/30	2.60	0.016	HSPA5	Heat shock 70kDa protein 5	9q33-q34.1	5.07	69977
	171	98	2/2	2.60	0.016	DPP3	Dipeptidyl-peptidase 3	11q12-13.1	5.01	82537
Metabolism; Energy pathways	804	186	3/3	2.56	0.0045	ASNA1	ArsA arsenite transporter, ATP-binding, homologue 1	19q13.3	4.81	38636
	804	174	4/5	2.56	0.0045	SMS	Spermine synthase	Xp22.1	4.87	41110
	854	229	4/4	2.25	0.000068	TALDO1	Transaldolase 1	11p15.5-p15.4	6.36	37516
snRNP assembly	757	113	2/2	2.81	0.04	WDR77	WD repeat domain 77	1p13.2	5.03	36701
	894	282	5/5	2.40	0.046	STRAP	Serine/threonine kinase receptor associated protein	12p12.3	4.98	38413
Glutathione homeostasis *Biological process unknown*	1440	383	6/6	3.29	0.041	GGCT	Gamma-glutamylcyclotransferase	7p15-p14	5.07	20994
	1392	116	2/2	2.04	0.0042	C1orf123	Chromosome 1 open reading frame 123	1p32.3	4.93	18036
	1440	99	1/1	3.29	0.041	TPD52	Tumor protein D52	8q21	4.79	24312
Mitochondrial metabolism	1631	93	1/1	−2.26	0.023	ATP5D	ATP synthase, H + transporting, mitochondrial F1 complex, delta subunit	19p13.3	4.53	15010
	1392	184	4/6	2.04	0.0042	NDUFS8	NADH dehydrogenase iron-sulfur protein 8, mitochondrial	11q13	5.10	20276
Transport	1440	137	2/2	3.29	0.041	RAB1C	Ras-related protein Rab-1c	9p13.2	5.25	22017
	1440	135	2/2	3.29	0.041	RAB15	Ras-related protein Rab 15	14q23.3	5.35	24,391
Cytoskeleton	854	99	2/2	2.25	0.000068	SEPT11	Septin 11	4q21.1	6.38	49236

with trypsin (Promega, sequencing grade), essentially as described by Wilm *et al.* (7). Nanoflow LC-MS/MS was performed on an 1100 series capillary LC system (Agilent Technologies) coupled to an LTQ linear ion trap mass spectrometer (Thermo) operating in positive mode and equipped with a nanospray source. Peptide mixtures were trapped on a ReproSil C18 reversed phase column (Dr Maisch GmbH; column dimensions 1.5 cm $\times$100 µm, packed in-house) at a flow rate of 8 µl/min. Peptide separation was performed on ReproSil C18 reversed phase column (Dr Maisch GmbH; column dimensions 15 cm $\times$ 50 µm, packed in-house) using a linear gradient from 0 to 80% B (A = 0.1% formic acid; B = 80% (v/v) acetonitrile, 0.1% formic acid) in 70 min and at a constant flow rate of 200 nl/min using a splitter. The column eluent was directly sprayed into the ESI source of the mass spectrometer. Full mass spectra were acquired in continuum mode, while fragmentation spectra were acquired in centroid mode; fragmentation of the peptides was performed in data-dependent mode. Peak lists were automatically created from raw data files using the Mascot Distiller software (version 2.1; MatrixScience). The Mascot search algorithm (version 2.2, MatrixScience) was used to search against the Uniprot database. The peptide tolerance was typically set at 2 Da and the fragment ion tolerance was set at 0.8 Da. A maximum number of 2 missed cleavages by trypsin were allowed and carbamidomethylated cysteine and oxidised methionine were set as fixed and variable modifications, respectively. Based on a 95% confidence level, the identity threshold for each of the searches was 42. Taking at least two high-confidence peptides as a further criterion, the Mascot score cut-off value for a positive protein hit was set at 84. Proteins identified with only one high-confidence peptide were discarded, unless the identified proteins in the same spot showed generally low Mascot scores and the protein was "interesting": then the mass spectra were inspected manually (Supplementary Table S3 for an overview of all proteins identified; Supplementary File 1 for MS/MS spectra of proteins identified with one peptide). The final selection as presented in Table 2 was based on whether proteins were identified in many other protein spots (aspecific), whether the pI and molecular weight of the identified protein was in line with the corresponding protein spot and the Mascot score/number of unique peptides of the identified protein. Uniprot was used for functional classification of the proteins (www.uniprot.org).

Western blotting

For Western blotting, anterior horn homogenates of 9 ALS and 9 control cases were taken from the same samples used for proteomics, and the differences between control and ALS groups were statistically analysed by a Mann-Whitney test. For one ALS sample, insufficient material was available for further validation. ATP5D antibody (rabbit polyclonal, ab97491) and Calmodulin antibody (rabbit polyclonal, ab45689) were both purchased from Abcam. Western blotting was performed as reported previously (8, 9).

Immunohistochemistry and immunofluorescence

For immunohistochemistry FFPE, 5-µm-thick sections were deparaffinised and rehydrated in graded ethanol. After blockage of endogenous peroxidase activity with 3% H_2O_2, antigen retrieval was performed (10 minutes autoclaving in 10µM sodium citrate) and slides were incubated with a given primary antibody. The ATP5D and Calmodulin antibodies were the same as those used for immunoblotting; Synaptophysin antibody (mouse monoclonal SY38) was purchased from Dako; Glial fibrillary acidic protein mouse monoclonal antibody was purchased from Sigma. Antibody detection was performed using diaminobenzine (DAB) or Vector Red/Vector Blue system (Vector laboratories, Burlingame, CA). For immunofluorescence, sections of 6-7 µm were deparaffinated in xylene, rinsed in ethanol (100%, 95%, 70%) and incubated for 20 min in 0.3% hydrogen peroxide diluted in methanol. Antigen retrieval was performed using a pressure cooker in 0.01 M citrate buffer pH 6.0 at 120 °C for 10 min. Slides were washed with phosphate-buffered saline (PBS; 0.1 M, pH 7.4) and incubated overnight with the primary antibody in PBS at 4 °C. Section were then incubated for 2h at room temperature with Alexa Fluor® 568-conjugated anti-rabbit and Alexa Fluor® 488 anti-mouse IgG or anti-goat IgG (1:100, Molecular Probes, The Netherlands). Sections were analysed by means of a laser scanning confocal microscope (Leica TCS Sp2, Wetzlar, Germany).

Results

Differential protein analysis in ALS

To identify proteomic changes that occur in ALS, we analysed differential protein expression in spinal cord samples of sporadic ALS patients and controls using 2D-DIGE combined with mass spectrometry. Proteins were extracted from anterior and posterior horn samples that were isolated using a skin biopsy punch (Figure 1). Next, ALS samples were labelled with a green fluorescent dye (Cy3) and control samples with a red fluorescent dye (Cy5) or vice versa. Then, randomly paired samples were combined and separated in 2D-gels together with a Cy2-labelled internal standard, a pooled sample of all experimental samples that allows for comparison

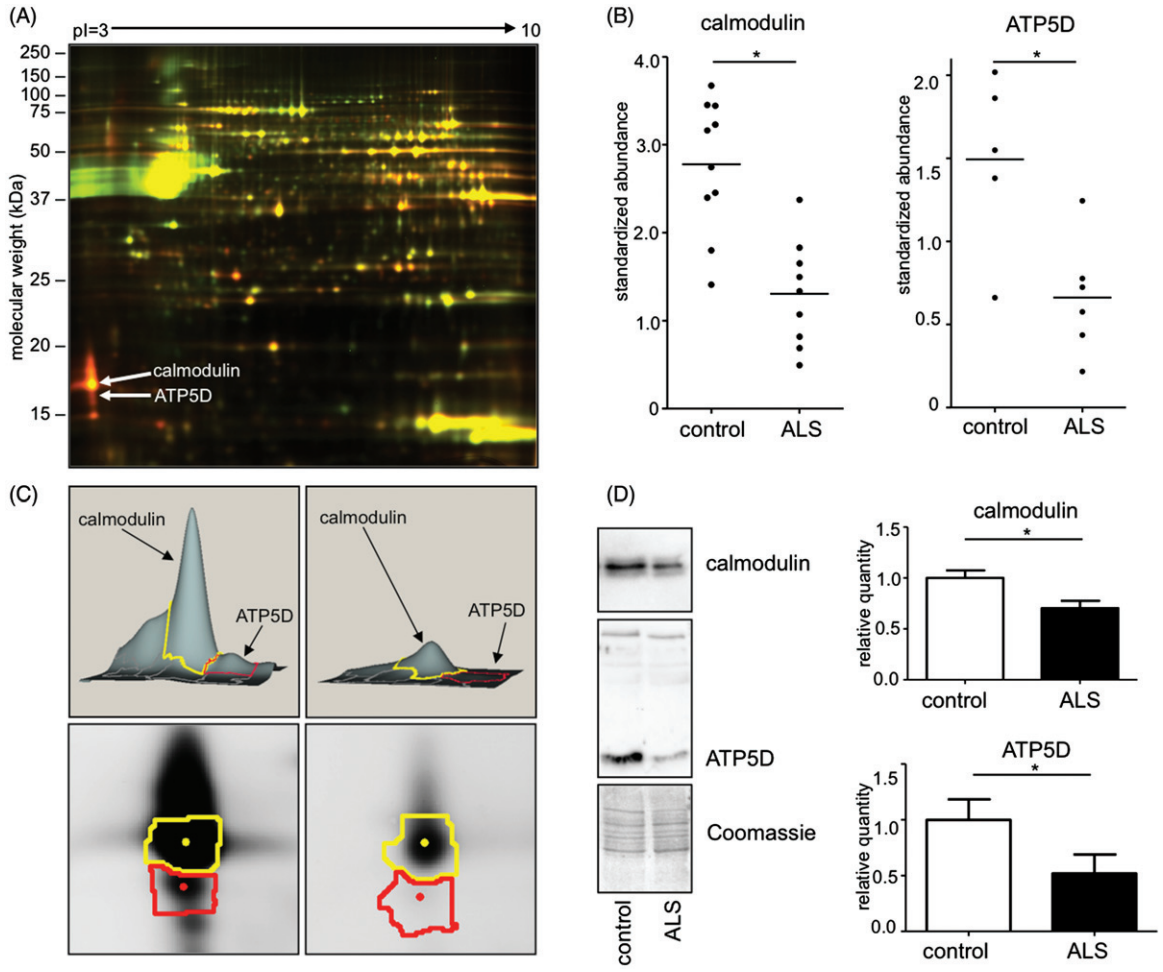

Figure 2. (A) A representative 2D-DIGE gel of anterior horn samples from a control and an ALS patient (100 μg per sample) labelled with red or green fluorescent dye, respectively. Samples were combined and separated by 2D gel electrophoresis. Protein spots shared between the 2 samples appear yellow and represent the unaffected proteome. Protein spots that are relatively less abundant in ALS are red, and relatively upregulated spots in ALS appear green. These experiments were performed in 10 patients and controls, allowing adequate statistical analysis. (B) Calmodulin and ATP5D protein levels are relatively downregulated in the ALS group compared to controls. Each dot represents 1 patient. $^{*}p<0.05$. (C) Representative gel images of calmodulin, ATP5D and Coomassie staining in one control (left) and one ALS patient (right). (D) Western blotting of ATP5D confirmed that ATP5D protein levels are decreased in the anterior horn of samples from the ALS group ($p=0.025$). Western blotting of calmodulin also showed a clear reduction of protein levels in the ALS group ($p=0.009$). Data are presented as mean ± SEM, $n=9$ per condition.

between gels (see Supplementary Table 1 for an overview of sample combinations and Cy-labels). Figure 2(A) shows a representative example of an ALS and control anterior horn sample; yellow spots indicate no differential protein expression; red spots represent relative downregulated proteins and green spots relative upregulated proteins in ALS compared to control. 1387 proteins were resolved for further analysis, 32 of which appeared to be differentially expressed (about 2.3%; log peak volume change >2.0- fold, protein detected in at least 3 patients, $p<0.05$). Of these 32 proteins, 27 proteins showed upregulation and 5 proteins downregulation in ALS samples. In contrast, comparison of the protein profiles of posterior horns of ALS patients and controls showed a significant difference for only 3 spots: all proteins were upregulated indicating that the proteomic changes identified are specific for the disease-affected-region.

Mitochondrial function, calcium homeostasis and protein metabolism are altered in ALS

A separate 'pick' gel was generated, which was loaded with a pooled sample of all experimental samples. Differential protein spots were isolated from this gel (Supplementary Table S1) and subjected to mass spectrometry. We identified 16 candidate proteins from the 27 protein spots with upregulation and 2 candidate proteins from the 5 spots with downregulation (Table 2). A functional classification of these proteins revealed that the identified proteins are involved in mitochondrial function (oxidative phosphorylation), intracellular calcium homeostasis, protein metabolism,

Table 3. Overview of proteins with significant level changes in the posterior horn of ALS; upregulated proteins have a positive, and downregulated negative log2 fold change values, respectively.

Biological process	Spot no.	Mascot score	Number of unique peptides/total peptides	Log2 fold change (ALS/controls)	T-test p-value	Gene symbol	Protein name	Chromosome locus	pI	Mw
Protein metabolism	171	1641	25/30	2.84	0.019	HSPA5	Heat shock 70kDa protein 5	9q33-q34.1	5.07	69977
	171	98	2/2	2.84	0.019	DPP3	dipeptidyl-peptidase 3	11q12-13.1	5.01	82537
Cell communication; Signal transduction	580	239	3/3	2.01	0.025	ST13	suppression of tumorigenicity 13 (colon carcinoma) (Hsp70 interacting protein)	22q13.2	5.18	41305

glutathione homeostasis, protein transport and snRNP assembly. Mass spectrometry analysis of the posterior horn tissue of the ALS and controls did not show gross changes and identified only 3 candidate proteins from 3 spots with upregulation, as summarised in Table 3. These proteins play a role in protein metabolism and probably reflect reactive processes in the posterior horn. Therefore, we did not follow-up on the posterior horn changes.

ATP5D and Calmodulin are downregulated in ALS

As the anterior horn changes are expected to reflect disease-specific alterations, we decided to look further into ATP5D and calmodulin, the two proteins that were downregulated in ALS (Figure 2B,C). Western blot analysis of ATP5D confirmed that ATP5D protein levels are decreased in the anterior horn of samples from the ALS group ($p = 0.025$) (Figure 2D). Western blotting of calmodulin also showed a clear reduction of protein levels in the ALS group ($p = 0.009$) (Figure 2D). We also performed immunoblotting for two upregulated hits, CHP and HSPA5, but protein levels did not appear to be significantly altered (data not shown).

To further validate our findings, we performed single immunohistochemical staining of ATP5D on ALS and control spinal cord tissue and found decreased expression of ATP5D, mainly in the extraneuronal background, as shown in Figure 3(A). With regard to calmodulin, a single immunohistochemical staining showed diffusely decreased calmodulin expression in both neuronal bodies and dendrites (Figure 4). Hence, with regard to these two downregulated proteins, we could confirm their downregulation using both Western blot and immunohistochemical staining, thereby validating our approach.

ATP5D is specifically downregulated at the synapse

Because ATP5D expression seemed to be downregulated in the extraneuronal space only, we wondered whether this occurs at synaptic sites or mainly in non-neuronal cells. We, therefore, performed a double staining with ATP5D and synaptophysin (a synaptic marker) and found a marked decrease of ATP5D specifically at synaptic sites in ALS compared to control (Figures 3B and C). In contrast, a double staining of ATP5D and glial fibrillary acidic protein (GFAP), a marker for glial cells, indicated that ATP5D and GFAP do not colocalize and that the downregulation of ATP5D is likely to be specific for neuronal cells. When performing a double immunofluorescence staining for calmodulin and synaptophysin, there seemed to be a decrease of calmodulin expression mainly in neuronal bodies and dendrites, although these differences were less clear (Figure 4).

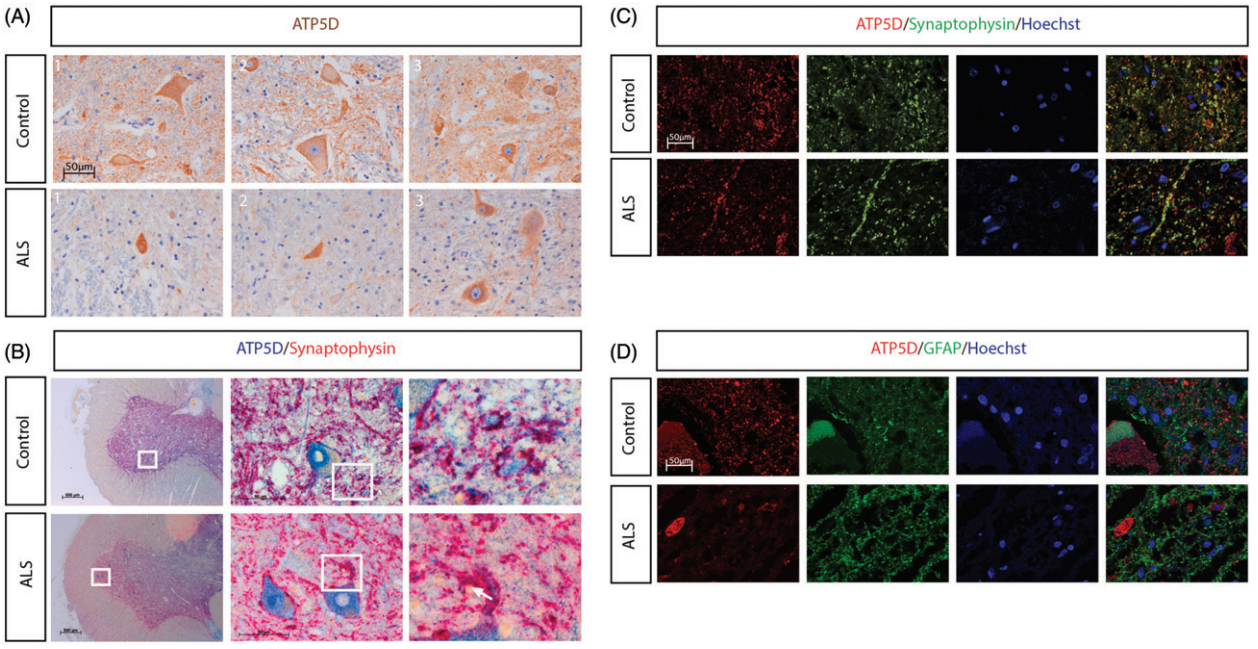

Figure 3. (A) Single immunohistochemical staining of ATP5D shows decreased staining in the anterior horn of ALS cases (lower panel) compared to control subjects (upper panel), mainly in the extra-neuronal region. (B) Synaptophysin (red)/ATP5D (blue) double immunohistochemical staining of anterior spinal cord of an ALS case and a control. The red synaptophysin stain represents neuronal body, axons and dendrites. The double staining shows decreased ATP5D staining at synaptic sites (white arrow), whereas in a control case, ATP5D shows synaptic localisation (upper panel). (C) Synaptophysin (green)/ATP5D (red) immunofluorescent double staining again shows loss of ATP5D at synaptic sites in ALS. The blue dots represent nuclei. (D) Glial fibrillary acidic protein (GFAP) (green) and ATP5D (red) immunofluorescent double staining shows no colocalization between ATP5D and GFAP in a control case, indicating that the observed loss of ATP5D in ALS is not in glial cells, but neuron-specific.

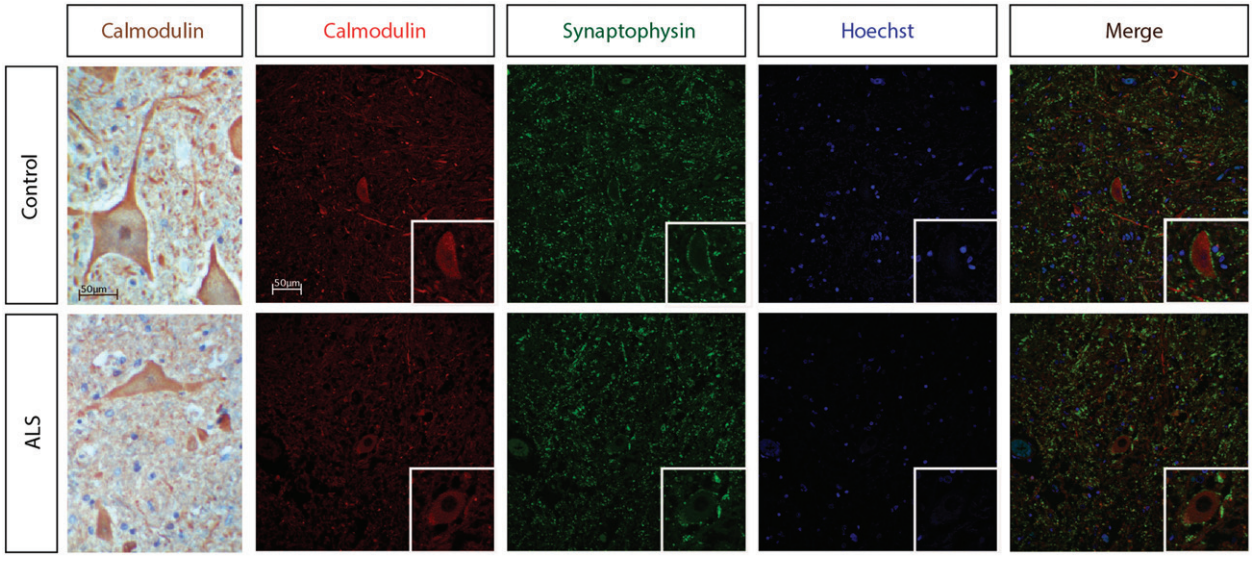

Figure 4. (Far left panels) Calmodulin single immunohistochemical staining shows diffuse cytoplasmic staining of neuronal bodies, axons and dendrites. The control shows more intense calmodulin stain in the extra-neuronal space than the ALS. (Right panels) Calmodulin (red)/synaptophysin (green) double immunofluorescent staining of spinal cord anterior horn of an ALS case and a control. The intensity of calmodulin staining appears to be less in neuronal bodies and dendrites, although the decrease in protein expression is less substantial than observed for ATP5D.

Discussion

We performed a fluorescent 2D-DIGE proteomic analysis combined with MS using post-mortem spinal cord of human ALS patients and controls. The anterior horn of the ALS group showed 18 proteins with significant level changes compared to the control group, in contrast to only 3 differentially expressed proteins in the posterior horns. This suggests that the identified proteins in the anterior horn are specific and potentially relevant in the pathogenesis of sALS. A functional classification of

the proteomic changes associated with ALS showed involvement in mitochondrial function (oxidative phosphorylation), intracellular calcium homeostasis, protein metabolism, glutathione homeostasis, protein transport and snRNP assembly.

There have been earlier attempts to establish protein profiles of ALS, mostly in CSF to identify biomarkers (10–18), in muscle of ALS patients (19, 20) or in spinal cord material derived from animal models (21–25). Our study used spinal cord tissue from human sALS patients and control subjects for proteomic profiling, which is expected to identify proteins directly relevant to the disease. Only one previous study investigated ALS protein profiles in human spinal cord material. That study used MALDI imaging spatial protein profiling in 4 ALS patients and 3 control subjects and was limited to proteins smaller than 20–30 kDa (26). One protein was identified to be differentially expressed in ALS, namely a truncated form of ubiquitin (Ubs-T). In our study Ubs-T was not found to be differentially expressed, probably due to a difference in experimental setup.

Although thousands of proteins can be resolved from a single gel using 2D gel electrophoresis, proteins of extreme size, like Ubs-T (8.5 kDa) or charge or with very low abundance cannot be detected. Furthermore, some of the resolved proteins are not identified by tandem MS. Moreover, although the uniqueness of our study lies in the use of patient-derived spinal cord material, the downfall of this approach is that the material reflects the end-stage of the disease. It is therefore uncertain whether the identified proteomic alterations are directly related to the disease or more generally involved in cell death or gliosis.

While a decreased level of many proteins was expected in ALS, as a result of decreased number and atrophy of motor neurons, of the 22 differently expressed proteins, only two proteins were downregulated - ATP5D and calmodulin. This intriguing finding invited further investigation. Western blotting, immunohistochemistry and immunofluorescence validated the downregulation of ATP5D and calmodulin. Immunohistochemistry results indicated that loss of ATP5D in ALS was most pronounced at synaptic sites along the axons and dendrites.

The reduced expression of ATP5D protein in ALS patients is in line with two earlier independent studies reporting downregulation of the ATP5D transcript, one studying expression profiles of spinal cord grey matter of ALS patients (27) and one studying expression profiles in the SOD1 mouse model of ALS (24). ATP5D is a subunit of ATP synthase, a mitochondrial protein complex essential for ATP production; knockdown of ATP5D results in reduced levels of ATP synthase (28–30). Interestingly, swollen and vacuolated mitochondria have been described to be present in motor neurons and muscle tissue in ALS samples (31).

We also found reduced levels of calmodulin in the ALS group. A decreased level of calmodulin suggests disruption of calcium homeostasis. Interestingly, perturbed calcium buffering has been associated with motor neuron impairment (32). Furthermore, in various studies, calcium overload has been shown to be damaging to mitochondria, possibly due to increase in reactive oxygen species (33).

Proteomic analysis is a rapidly developing technique, but still faces challenges such as uniformity of peptide digestion, detection of low-abundant proteins and completeness of MS analysis (34). Furthermore, our study covered only quantitative differences, while posttranslational modifications, such as phosphorylation, acetylation, methylation, glycosylation or ubiquitination may also play an important role in the disease. Since a large quantity of protein was required for this analysis, we extracted protein from the anterior horn region containing both motor neurons and glial cells, instead of obtaining isolated motor neurons by microdissection. This 'second best' approach turned out to be advantageous, revealing abnormal protein levels primarily located at synaptic sites.

We show that proteomic profiling of spinal cord material of sporadic ALS cases can provide insights into ALS disease pathogenesis. It would be interesting to know whether the proteomic differences observed in this study reflect alterations in transcription or translation. Therefore, future studies could perform transcriptomic profiling of the spinal cord in ALS. Furthermore, it will be of great interest to investigate whether proteomic profiles of patients carrying specific mutations, e.g. C9orf72 mutation carriers, show comparable proteomic changes or display mutation-specific alterations. This is of special interest as evidence is accumulating that pathological profiles are distinct between different ALS-associated mutation carriers, e.g. the TDP-43-negative, p62- UBLQN-positive inclusions in hippocampus, frontotemporal neocortex and cerebellum that contain dipeptide repeat proteins and distinguish C9orf72 expanded repeat from non-expanded repeat carriers (35, 36). This could provide more insight into the disease pathogenesis and open avenues for therapeutic approaches.

Declaration of interest

L.H.v.d.B. received an educational grant from Baxter International Inc., and served on a scientific advisory board of Biogen Idec and Cytokinetics. This work was supported by funding from the Prinses Beatrix Spierfonds, the Netherlands Organisation for Health Research and Development (ZonMW-VICI: L.H.v.d.B), the Netherlands ALS Foundation, and The European

Community's Health Seventh Framework Programme [grant agreement no. 259867].

References

1. Ferraiuolo L, Kirby J, Grierson AJ, Sendtner M, Shaw PJ. Molecular pathways of motor neuron injury in amyotrophic lateral sclerosis. Nat Rev Neurol. 2011;7:616–30.
2. Al-Chalabi A, Jones A, Troakes C, King A, Al-Sarraj S, van den Berg LH. The genetics and neuropathology of amyotrophic lateral sclerosis. Acta Neuropathol. 2012;124:339–52.
3. Blokhuis AM, Groen EJN, Koppers M, van den Berg LH, Pasterkamp RJ. Protein aggregation in amyotrophic lateral sclerosis. Acta Neuropathol. 2013;125:777–94.
4. Robberecht W, Philips T. The changing scene of amyotrophic lateral sclerosis. Nat Rev Neurosci. 2013;14:248–64.
5. Bovenschen N, Quadir R, van den Berg AL, Brenkman AB, Vandenberghe I, Devreese B, et al. Granzyme K displays highly restricted substrate specificity that only partially overlaps with granzyme A. J Biol Chem. 2009;284:3504–12.
6. Alban A, David SO, Bjorkesten L, Andersson C, Sloge E, Lewis S, et al. A novel experimental design for comparative two-dimensional gel analysis: two-dimensional difference gel electrophoresis incorporating a pooled internal standard. Proteomics. 2003;3:36–44.
7. Wilm M, Shevchenko A, Houthaeve T, Breit S, Schweigerer L, Fotsis T, et al. Femtomole sequencing of proteins from polyacrylamide gels by nano-electrospray mass spectrometry. Nature. 1996;379:466–9.
8. Groen EJN, Fumoto K, Blokhuis AM, Engelen-Lee J, Zhou Y, van den Heuvel DMA, et al. ALS-associated mutations in FUS disrupt the axonal distribution and function of SMN. Hum Mol Genet. 2013;22:3690–704.
9. Koppers M, Blokhuis AM, Westeneng HJ, Terpstra ML, Zundel CA, Vieira de Sa R, et al. C9orf72 ablation in mice does not cause motor neuron degeneration or motor deficits. Ann Neurol. 2015;78:426–38.
10. Zhou J-Y, Afjehi-Sadat L, Asress S, Duong DM, Cudkowicz M, Glass JD, et al. Galectin-3 Is a candidate biomarker for amyotrophic lateral sclerosis: discovery by a proteomics approach. J Proteome Res. 2010;9:5133–41.
11. Brettschneider J, Mogel H, Lehmensiek V, Ahlert T, Süssmuth S, Ludolph AC, et al. Proteome analysis of cerebrospinal fluid in amyotrophic lateral sclerosis (ALS). Neurochem Res. 2008;33:2358–63.
12. Dengler R, von Neuhoff N, Bufler J, Krampfl K, Peschel T, Grosskreutz J. Amyotrophic lateral sclerosis: new developments in diagnostic markers. Neurodegener Dis. 2005;2:177–84.
13. Ryberg H, An J, Darko S, Lustgarten JL, Jaffa M, Gopalakrishnan V, et al. Discovery and verification of amyotrophic lateral sclerosis biomarkers by proteomics. Muscle Nerve. 2010;42:104–11.
14. von Neuhoff N, Oumeraci T, Wolf T, Kollewe K, Bewerunge P, Neumann B, et al. Monitoring CSF proteome alterations in amyotrophic lateral sclerosis: obstacles and perspectives in translating a novel marker panel to the clinic. PLoS One. 2012;7:e44401.
15. Häggmark A, Mikus M, Mohsenchian A, Hong M-G, Forsström B, Gajewska B, et al. Plasma profiling reveals three proteins associated to amyotrophic lateral sclerosis. Ann Clin Transl Neurol. 2014;1:544–53.
16. Pasinetti GM, Ungar LH, Lange DJ, Yemul S, Deng H, Yuan X, et al. Identification of potential CSF biomarkers in ALS. Neurology. 2006;66:1218–22.
17. Ramstrom M, Ivonin I, Johansson A, Askmark H, Markides KE, Zubarev R, et al. Cerebrospinal fluid protein patterns in neurodegenerative disease revealed by liquid chromatography-Fourier transform ion cyclotron resonance mass spectrometry. Proteomics. 2004;4:4010–8.
18. Ranganathan S, Williams E, Ganchev P, Gopalakrishnan V, Lacomis D, Urbinelli L, et al. Proteomic profiling of cerebrospinal fluid identifies biomarkers for amyotrophic lateral sclerosis. J Neurochem. 2005;95:1461–71.
19. Elf K, Shevchenko G, Nygren I, Larsson L, Bergquist J, Askmark H, et al. Alterations in muscle proteome of patients diagnosed with amyotrophic lateral sclerosis. J Proteomics. 2014;108:55–64.
20. Yin F, Ye F, Tan L, Liu K, Xuan Z, Zhang J, et al. Alterations of signalling pathways in muscle tissues of patients with amyotrophic lateral sclerosis. Muscle Nerve. 2012;46:856–60.
21. Massignan T, Casoni F, Basso M, Stefanazzi P, Biasini E, Tortarolo M, et al. Proteomic analysis of spinal cord of presymptomatic amyotrophic lateral sclerosis G93A SOD1 mouse. Biochem Biophys Res Commun. 2007;353:719–25.
22. Zhai J, Ström A-L, Kilty R, Venkatakrishnan P, White J, Everson WV, et al. Proteomic characterization of lipid raft proteins in amyotrophic lateral sclerosis mouse spinal cord. FEBS J. 2009;276:3308–23.
23. Duplan L, Bernard N, Casseron W, Dudley K, Thouvenot E, Honnorat J, et al. Collapsin Response mediator protein 4a (CRMP4a) is upregulated in motoneurons of mutant SOD1 mice and can trigger motoneuron axonal degeneration and cell death. J Neurosci. 2010;30:785–96.
24. Ferraiuolo L, Heath PR, Holden H, Kasher P, Kirby J, Shaw PJ. Microarray analysis of the cellular pathways involved in the adaptation to and progression of motor neuron injury in the SOD1 G93A mouse model of familial ALS. J Neurosci. 2007;27:9201–19.
25. Acquadro E, Caron I, Tortarolo M, Bucci EM, Bendotti C, Corpillo D. Human SOD1-G93A specific distribution evidenced in murine brain of a transgenic model for amyotrophic lateral sclerosis by MALDI imaging mass spectrometry. J Proteome Res. 2014;13:1800–9.
26. Hanrieder J, Ekegren T, Andersson M, Bergquist J. MALDI imaging of post-mortem human spinal cord in amyotrophic lateral sclerosis. J Neurochem. 2013;124:695–707.
27. Dangond F. Molecular signature of late-stage human ALS revealed by expression profiling of postmortem spinal cord gray mattermortem. Physiol Genomics. 2003;16:229–39.
28. Duvezin-Caubet S, Rak M, Lefebvre-Legendre L, Tetaud E, Bonnefoy N, di Rago JP. A petite obligate mutant of Saccharomyces cerevisiae: functional mtDNA is lethal in cells lacking the delta subunit of mitochondrial F1-ATPase. J Chem. 2006;281:16305–13.
29. Geisler DA, Papke C, Obata T, Nunes-Nesi A, Matthes A, Schneitz K, et al. Downregulation of the -subunit reduces mitochondrial ATP synthase levels, alters respiration, and restricts growth and gametophyte development in arabidopsis. Plant Cell. 2012;24:2792–811.
30. Hilbers F, Eggers R, Pradela K, Friedrich K, Herkenhoff-Hesselmann B, Becker E, et al. Subunit δ is the key player for assembly of the H(+)-translocating unit of Escherichia coli F(O)F1 ATP synthase. J Biol Chem. 2013;288:25880–94.
31. Cozzolino M, Ferri A, Valle C, Carrì MT. Mitochondria and ALS: implications from novel genes and pathways. Mol Cell Neurosci. 2013;55:44–9.
32. Jaiswal MK. Selective vulnerability of motoneuron and perturbed mitochondrial calcium homeostasis in amyotrophic lateral sclerosis: implications for motoneurons specific calcium dysregulation. Mol Cell Ther. 2014;2:15.
33. Peng T-I, Jou M-J. Oxidative stress caused by mitochondrial calcium overload. Ann NY Acad Sci. 2010;1201:183–8.
34. Cox J, Mann M. Is proteomics the new genomics? Cell. 2007;130:395–8.

35. Al-Sarraj S, King A, Troakes C, Smith B, Maekawa S, Bodi I, et al. p62 positive, TDP-43 negative, neuronal cytoplasmic and intranuclear inclusions in the cerebellum and hippocampus define the pathology of C9orf72-linked FTLD and MND/ALS. Acta Neuropathol. 2011;122:691–702.

36. Brettschneider J, Deerlin VM, Robinson JL, Kwong L, Lee EB, Ali YO, et al. Pattern of ubiquilin pathology in ALS and FTLD indicates presence of C9ORF72 hexanucleotide expansion. Acta Neuropathol. 2012;123: 825–39.

Supplementary material available online